Atmos. Chem. Phys. Discuss., 13, 21003–21040, 2013
www.atmos-chem-phys-discuss.net/13/21003/2013/
doi:10.5194/acpd-13-21003-2013

Atmospheric Chemistry and Physics Discussions

Sulfur hexafluoride (SF_6) emissions in East Asia determined by inverse modeling

X. Fang[1,2], R. L. Thompson[1], T. Saito[3], Y. Yokouchi[3], J. Kim[4,5], S. Li[4,6], K. R. Kim[4,6], S. Park[7], F. Graziosi[8], and A. Stohl[1]

[1]Norwegian Institute for Air Research, Kjeller, Norway
[2]State Key Joint Laboratory for Environmental Simulation and Pollution Control, College of Environmental Sciences and Engineering, Peking University, Beijing, China
[3]National Institute for Environmental Studies, Tsukuba, Japan
[4]School of Earth and Environmental Sciences, Seoul National University, Seoul, South Korea
[5]Scripps Institution of Oceanography, University of California at San Diego, La Jolla, California, USA
[6]Research Institute of Oceanography, Seoul National University, Seoul, South Korea
[7]Department of Oceanography, Kyungpook National University, Sangju, South Korea
[8]University of Urbino, Urbino, Italy

Received: 4 June 2013 – Accepted: 25 July 2013 – Published: 13 August 2013

Correspondence to: X. Fang (fangxuekun@gmail.com)

Published by Copernicus Publications on behalf of the European Geosciences Union.

Abstract

Sulfur hexafluoride (SF_6) has a global warming potential of around 22 800 over a 100 yr time horizon and is one of the greenhouse gases regulated under the Kyoto Protocol. Around circa 2000 there was a reversal in the global SF_6 emission trend, from a decreasing to an increasing trend, which was likely caused by increasing emissions in countries that are not obligated to report their annual emissions to the United Nations Framework Convention on Climate Change. In this study, SF_6 emissions during the period 2006–2012 for all East Asian countries, including Mongolia, China, the Taiwan region, North Korea, South Korea and Japan, were determined by using inverse modeling and in-situ atmospheric measurements. We found that the most important sources of uncertainty associated with these inversions are related to the choice of a priori emissions and their assumed uncertainty, the station network as well as the meteorological input data. Much lower uncertainties are due to seasonal variability in the emissions, inversion geometry and resolution, and the measurement calibration scale. Based on the results of these sensitivity tests, we estimate that the total SF_6 emission in East Asia increased rapidly from $2437 \pm 329\,Mg\,yr^{-1}$ in 2006 to $3787 \pm 512\,Mg\,yr^{-1}$ in 2009 and stabilized thereafter. China contributed 58–72 % to the total East Asian emission for the different years, followed by South Korea (9–19 %), Japan (5–16 %) and the Taiwan region (4–7 %), while the contributions from North Korea and Mongolia together were less than 3 % of the total. The per-capita SF_6 emissions are highest in South Korea and the Taiwan region, while the per-capita emissions for China, North Korea and Japan are close to global average. During the period 2006–2012, emissions from China increased rapidly and emissions from South Korea increased slightly, while emissions from the Taiwan region and Japan decreased overall.

ACPD
13, 21003–21040, 2013

1 Introduction

Sulfur hexafluoride (SF_6) is one of the six greenhouse gases (GHG) regulated under the Kyoto Protocol (UN, 1998). Its atmospheric lifetime is estimated to be ~ 3200 yr (Ravishankara et al., 1993). It is the most potent GHG with a global warming potential (GWP) of 22 800 over a 100 yr time horizon (Forster et al., 2007). The major source for SF_6 emissions to the atmosphere is high voltage electric equipment, but magnesium production, electronics manufacturing, SF_6 production and other sources also emit SF_6 (Olivier et al., 2005). Long-term atmospheric measurements show that the growth rate of the atmospheric SF_6 mole fraction has increased again since around the year 2000, after a small decrease in the period 1995–2000 (Rigby et al., 2010). An explanation for this behavior is that SF_6 emission reductions have been achieved in most of the developed countries that are obligated to report their annual emissions to the United Nations Framework Convention on Climate Change (UNFCCC; so-called "Annex I" countries). However, further emission reductions after the year 2000 could no longer compensate the increase in the emissions from countries not required to report their emissions due to their developing status (so-called "non-Annex I" countires; Levin et al., 2010; Rigby et al., 2010).

All countries in East Asia, except for Japan, are non-Annex I countries. Every year, the Greenhouse Gas Inventory Office of Japan (GIO) submits their emission estimates based on inventory technology to UNFCCC (GIO, 2012). Each non-Annex I country is required to submit its initial communication within three years of the entry into force of the Convention for that country (UN, 1998). The Second National Communication of South Korea submitted to UNFCC reports SF_6 emissions of around 700 $Mg\,yr^{-1}$ during the period 2006–2009 (Republic of Korea, 2012). The Second Communication for the Taiwan region reports SF_6 emissions of about 120 $Mg\,yr^{-1}$ within 2006–2008 (Taiwan, 2011). Mongolia and China only report emissions in 2005 of 0 $Mg\,yr^{-1}$ (Mongolia, 2010) and 436.7 $Mg\,yr^{-1}$ (China, 2012), respectively. SF_6 emissions are not included in North

ACPD
13, 21003–21040, 2013

Korea's Communication (Democratic People's Republic of Korea, 2000). These bottom-up national estimates, however, are uncertain and need independent validation.

Top-down estimates based on atmospheric SF_6 measurements provide one way to validate these inventories. Based on measurements from the Shangdianzi station in China and a Lagrangian transport model, SF_6 emissions from China were estimated for the first time to be 800 (530–1100) $Mg\,yr^{-1}$ in October 2006–March 2008 (Vollmer et al., 2009). SF_6 emissions were estimated for South Korea, China and Japan during November 2007 to December 2008 based on an inter-species ratio method and atmospheric measurements at the Gosan station in Korea (Li et al., 2011; Kim et al., 2010). Using combined Eulerian and Lagrangian chemical transport models and measurement data from Gosan, average emissions for the period 2007–2009 were estimated for South Korea, China, Japan and the Taiwan region (Rigby et al., 2011). In some cases, discrepancies are found among these top-down estimates and the bottom-up inventories. For example, emissions from South Korea for 2008 were estimated to be 380 (330–440) $Mg\,yr^{-1}$ (Li et al., 2011), 221 (154–287) $Mg\,yr^{-1}$ (2007–2009 average, Rigby et al., 2011) and 728 $Mg\,yr^{-1}$ (Republic of Korea, 2012).

In this study, we quantify the emissions in East Asia during the last seven years (2006–2012) using measurement data from several stations in this region, a Lagrangian particle dispersion model, and inverse modeling.

2 Methodology

2.1 Measurement data

In this study, we used in-situ measurements from three stations in East Asia and from two stations outside East Asia (Table 1). The Asian stations are: (1) Gosan, situated on Jeju Island in the Yellow Sea south of the Korean peninsula and is operated by the Seoul National University (SNU), Korea (Kim et al., 2010), as part of the Advanced Global Atmospheric Gases Experiment (AGAGE) global network, (2) Hateruma, lo-

ACPD
13, 21003–21040, 2013

cated on a small island with an area of 12.7 km^2 at the southern edge of the Japanese archipelago, and (3) Cape Ochi-ishi, at the tip of the Nemuro Peninsula located in the eastern part of Hokkaido, Japan. Both Japanese stations are operated by the National Institute for Environmental Studies (NIES; Tohjima et al., 2002).

At Gosan, ambient mixing ratios of SF_6 are measured every two hours using the "Medusa-Gas Chromatograph Mass Spectrometry (GC-MS)" technology (Miller et al., 2008). Measurements of SF_6 started in November 2007 but only data from January 2008 were used here. At Hateruma and Cape Ochi-shi stations, SF_6 mixing ratios are measured once per hour using a technique developed at NIES based on cryogenic preconcentration and a capillary GC-MS (Enomoto, 2005; Yokouchi et al., 2006). The Japanese measurements are reported on the NIES-2008 calibration scale, whereas for the other stations the SIO-2005 calibration scale was used. Intercomparisons between the NIES-2008 and SIO-2005 scales yielded NIES-2008/SIO-2005 ratio of 1.013 ± 0.006. We used this value to convert all NIES data from the NIES-2008 to the SIO-2005 calibration scale. Sensitivity tests demonstrate that using the NIES-2008 calibration scale as a reference increased the national emissions from all East Asian countries by less than 1.1 %, and that the differences in emissions were even smaller when SIO-2005 referenced data were adjusted to the widely used scale, NOAA-2006, by multiplication by a constant factor of 1.002 derived from Rigby et al. (2010), which will not be discussed any further.

Although this study only focuses on emissions in East Asia, we also used measurement data from the AGAGE stations Mace Head, Ireland and Trinidad Head, USA (Prinn et al., 2000). These two stations are operated by Atmospheric Chemistry Research Group, University of Bristol (UB), UK and Scripps Institution of Oceanography (SIO), University of California, USA, respectively. Tests show that national emissions for all East Asian countries differ by less than 2.0 % when not using these data.

ACPD
13, 21003–21040, 2013

2.2 Lagrangian backward modeling

The method of Lagrangian backward modeling used here is very similar to that presented in previous work (Stohl et al., 2009, 2010). Therefore, we only provide a brief description of the method here. The Lagrangian particle dispersion model FLEXPART v-9.02 (Stohl et al., 2005, 1998; http://www.flexpart.eu), was run every three hours for 20 days backwards in time to establish source–receptor relationships (SRR, often also called "footprint" or "emission sensitivity") between potential SF_6 emission sources and the change in mixing ratio at each measurement station.

FLEXPART was driven by operational 3 hourly meteorological data at $1^\circ \times 1^\circ$ resolution from the European Centre for Medium-Range Weather Forecasts (ECMWF) from 2006 to 2012. Figure 1 shows maps of average emission sensitivities for each station as well as for all stations combined for the period 2006–2012. North Korea, South Korea, Japan, the Taiwan region and most parts of China are well covered by the emission sensitivities of these three stations, which means that influence of emissions from these countries should be seen in the measured mixing ratios. Western and southwestern China is not well covered, however, this region is only sparsely populated and emissions there are expected to be small. There is minimal sensitivity to emissions over Southeast Asian countries, e.g., Vietnam, Malaysia, Philippines, and practically no sensitivity to emissions in South Asia, e.g., India, so these countries are not considered in this study.

To determine how sensitive our results are on the choice of the meteorological input data used for driving FLEXPART, we made alternative simulations for the year 2008 driven with $0.25^\circ \times 0.25^\circ$ 3 hourly nested ECMWF data, $1^\circ \times 1^\circ$ 6 hourly National Center for Environmental Prediction (NCEP) Final Analyses (FNL) Operational Model Global Tropospheric Analyses data (http://rda.ucar.edu/datasets/ds083.2/) and $0.5^\circ \times 0.5^\circ$ 3 hourly NCEP Climate Forecast System Reanalysis (CFSR) 6 hourly products (http://rda.ucar.edu/datasets/ds093.0/).

ACPD
13, 21003–21040, 2013

2.3 Inversion routine

The inversion method used is the same as described and evaluated by Stohl et al. (2009, 2010). Briefly, a Bayesian optimization technique is employed to estimate both emission strength and distribution over the domain influencing the measurement sites. The algorithm optimizes the model agreement with the measurements, while also considering a priori emissions and the uncertainties in the emissions, observations and the model simulations. The cost function to be minimized is:

$$J = (\mathbf{M}\widetilde{x} - \widetilde{y})^T \mathrm{diag}(\sigma_o^{-2})(\mathbf{M}\widetilde{x} - \widetilde{y}) + \widetilde{x}^T \mathrm{diag}(\sigma_x^{-2})\widetilde{x} \quad (1)$$

where σ_o is the vector of errors in the observation space (including the model error), σ_x is the vector of errors of the state space (i.e. in the a priori emissions), **M** represents the SRR matrix determined by the FLEXPART backward simulations, $\widetilde{x}$ is the difference between the a posteriori and a priori emission vectors, and $\widetilde{y}$ is the difference between observed mixing ratio vector and that simulated a priori, respectively. We used the same mixing ratio baseline filtering method as described in detail by Stohl et al. (2009), which also includes an optimization of the baseline by the inversion scheme. A variable-resolution emission grid, with grid sizes ranging from $18^\circ \times 18^\circ$ to $0.5^\circ \times 0.5^\circ$ was used for the inversion. A zoom-in over the East Asian part of the global variable-resolution grid used for the inversion is shown in Fig. 2.

2.4 A priori information

In this study, we use the average value of two previous estimates of global SF6 emissions for the years 2006–2008 and linearly extrapolate the emissions to 2012 using the trend for the years 2004–2008. The two previous estimates are: 6500, 7140 and 7420 $\mathrm{Mg\,yr^{-1}}$ for 2006, 2007 and 2008, respectively (Rigby et al., 2010) and 6290, 6790 and 7160 $\mathrm{Mg\,yr^{-1}}$ for the same years (Levin et al., 2010).

We collected all available information on emissions from individual countries. The latest available UNFCCC data for more than 40 countries are for 2010 (UNFCCC, 2012a),

ACPD
13, 21003–21040, 2013

and we assumed that emissions in 2011 and 2012 for each country were equal to an average of the corresponding emissions from 2008–2010. In East Asia, Japan is the only Annex I country and its reported emissions decrease from 205 $Mg\,yr^{-1}$ in 2006 to 78 $Mg\,yr^{-1}$ in 2010 (UNFCCC, 2012a; GIO, 2012). For South Korea, the Second National Communication reports emissions of 669, 707, 728 and 778 $Mg\,yr^{-1}$ from 2006 to 2009, respectively (Republic of Korea, 2012). Clean Development Mechanism (CDM) projects with a reduction target of 86 $Mg\,yr^{-1}$ were launched in 2010, with an additional reduction capacity of 64 $Mg\,yr^{-1}$ in 2011 (UNFCCC, 2012b), so we adopted a priori emissions of 692, 628 and 628 $Mg\,yr^{-1}$ from 2010 to 2012, respectively. For China, a priori information was derived from a comprehensive inventory for mainland China for 1990–2010 and a projection to 2020, which was recently made by compiling consumption and emission factor data for four industrial sources by Fang et al. (2013). For the Taiwan region, we adopted the values reported by the Second National Communication submitted to the UNFCCC (Taiwan, 2011), which are 125, 125 and 129 $Mg\,yr^{-1}$ for 2006, 2007 and 2008, respectively. They were extrapolated to 2012 by averaging the values for 2006–2008. All the national and global a priori emissions used in our study are listed in Table S1 in the Supplement. The remaining emissions in all other countries (including North Korea, for which little information is available) were disaggregated according to the Population Density Grid Future Estimates v3 for 2010 (CIESIN, 2005). This data set was also used for gridding all national emissions.

2.5 Quantification of national emissions

We defined a "reference" inversion that uses the best available a priori information (described in Sect. 2.4) and data from all stations. We performed twelve inversions with various changes made to this reference set-up and report the national annual emissions as the ensemble average result. The uncertainty of national emissions is estimated based on various sensitivity tests described in Sect. 3. Regarding the inversion ensemble, first we removed the additional a priori information on China, South Korea and Taiwan, and instead assign these countries' emissions proportional to their frac-

ACPD
13, 21003–21040, 2013

tion of the global population from non-Annex I countries (the "no East Asia information" inversion). We also replaced our reference a priori emission data set with the EDGAR inventory (the "EDGAR" inversion). Finally, we repeated the reference, no East Asia information and EDGAR inversions with the a priori emissions and their uncertainties set to 50 %, 100 %, 150 %, and 200 % of the value in the reference inversion. In this study, emissions from mainland China, Hong Kong and Macao were summed-up and abbreviated as emissions from "China".

As shown in Sect. 3.4, changes in the measurement network can lead to systematic increases or decreases in national emissions. In our measurement data set, Gosan data are not available for 2006 and 2007. Therefore, we also performed the inversions without Gosan for 2008–2012 and determined the relative differences to the full-dataset inversion. For most countries, the relative emissions biases are very similar for different years. To avoid an influence of missing Gosan data in 2006–2007 on reported trends, the mean relative bias of the inversions without Gosan to the full-station network case was removed for 2006–2007.

3 Sensitivity tests

The influence of various possible uncertainty factors on inversion performance was tested, and accordingly the resulting uncertainties of national a posteriori emissions were quantified. All sensitivity tests were done for the year 2008, for which we had a complete data set and alternative meteorological data available.

3.1 A priori information

We evaluated the influence of different a priori emission data sets on the inversion: (1) the reference data set, UNFCCC and East Asian country emissions were disaggregated using the CIESIN (2005) population map (UNFCCC/East Asia/CIESIN, or UC_adjust); (2) the same as UC_adjust but without East Asian country-specific infor-

ACPD
13, 21003–21040, 2013

mation (UNFCCC/CIESIN, or UC), and (3) the gridded SF_6 inventory from EDGAR v4.2 (termed EDGAR). Note that the emissions allocation in EDGAR is quite different from the CIESIN (2005) global population map, because EDGAR uses the urban settlements of CIESIN (2005) for an urban population map that was used as a proxy for spatial emission distribution (Janssens-Maenhout et al., 2013).

To evaluate the different a priori emission data sets, we compare the a priori model results with the station measurements. The mean bias between the a priori mixing ratios and observations (B_a) is the smallest for our reference data set UC_adjust (Table S2 in the Supplement). For example at Gosan, the bias is only 0.165 ppt, whereas corresponding biases with EDGAR and UC emissions are several times higher. The a priori root-mean-square errors (E_a) and the squared Pearson correlation coefficients between the observations and the a priori model results (r_a^2) values are lowest and highest, respectively, for UC_adjust at Gosan and Cape Ochi-ishi, but not at Hateruma, where the EDGAR simulation performs better. This is because for air masses crossing the Taiwan region, simulation results are best using the higher EDGAR emissions for the Taiwan region (Table S3 in the Supplement).

A posteriori emissions and distribution are a little different among UC_adjust, UC, and EDGAR inversions (Fig. S1 in the Supplement). Total a posteriori emissions for China are highest (2668 $Mg\,yr^{-1}$) in EDGAR inversion, while values for the UC_adjust and UC inversions are lower (2312 $Mg\,yr^{-1}$ and 2258 $Mg\,yr^{-1}$, respectively). The reason for this is the urban concentration of the emissions in the EDGAR dataset, which – due to the constant relative emission uncertainty scaling – also leads to very high emission uncertainties in a few grid boxes. This allowed the inversion (which increased Chinese emissions in all cases) to increase the emissions relatively more than with the more homogeneously distributed uncertainties in the other data sets, a non-linear effect of the concentration of high values of both the emissions and their uncertainties in a relatively small number of grid cells. While our statistical comparison of the model results and measurement data at Gosan and Cape Ochi-ishi was best for the UC_adjust case also for the a posteriori emissions, the EDGAR case was slightly better at Hateruma

ACPD
13, 21003–21040, 2013

(Table S2 in the Supplement). Therefore, averages of the a posteriori emissions from all three cases were used for reporting national emissions in Sect. 4.

3.2 Emission uncertainty

Uncertainties in the diagonal elements of $\boldsymbol{\sigma}_x$ in this study were defined like in Stohl et al. (2009), i.e., for inversion box j, $\boldsymbol{\sigma}_x^j = \max\langle p_1 x_j, p_2 x_{\text{surf}}\rangle$, with x_j being the a priori emission flux in inversion box j, x_{surf} the average land surface emission flux and p_1, p_2 appropriately chosen scaling factors. Stohl et al. (2009) used $p_1 = 0.4$ and $p_2 = 1.0$, with the first value slightly modified to $p_1 = 0.5$ by Stohl et al. (2010). Keller et al. (2011) used the same scaling factors as Stohl et al. (2009), while Keller et al. (2012) set both p_1 and p_2 to 3.0 for the hydrochlorofluorocarbons (HCFCs) and chlorofluorocarbons (CFCs), and to 1.0 for hydrofluorocarbons (HFCs) whose emissions compiled from the UNFCCC data are expected to be more accurate.

We tested the uncertainty scaling in a similar way as Keller et al. (2011) by employing $\boldsymbol{\sigma}_x^j = p \cdot \max\langle 0.5 x_j, 1.0 x_{\text{surf}}\rangle$, and varying the uncertainty scale factor p. The results in terms of a comparison of modeled and measured mixing ratios are shown in Fig. S2 in the Supplement. There is a nearly monotonic decrease in the root-mean-square errors (RMSE) and an increase in the correlation coefficient with increasing values of p, i.e., when the constraint to the a priori emissions is relaxed. However, there is hardly any change in the model skill for p values larger than 5. At the same time, the a posteriori emission maps show increasing levels of noise for these large p values, thus increasing the danger to retrieve artifacts as the a priori constraint is weakened. For instance, artificially high emissions for SF_6 were produced for $p > 5$ in southwestern China, which cannot be explained by known sources. The exact choice of the scale factor remains subjective, but from these tests a value of 1 appears most appropriate and was therefore used for our inversions.

ACPD
13, 21003–21040, 2013

3.3 Inversion resolution and geometry

A source of a posteriori emission errors in the country totals is the attribution of emissions in border regions to one of the neighboring countries. This is especially problematic for smaller countries like North and South Korea. A comparison of the a posteriori emissions when using 0.5° × 0.5° and 1° × 1° as the maximum grid resolution is shown in Fig. S3 in the Supplement. Differences are not systematic and, consequently, the total national a posteriori emissions do not change much for large countries. For example, a posteriori emissions for China and Japan differ by only 0 % and 1 % for these two inversions, respectively. However, for North Korea and South Korea, emissions are 28 % higher and −7 % lower with the coarser resolution, respectively. In this case, large emissions occur near the border between North and South Korea, and emissions are about ten times higher for South Korea than for North Korea. With the coarser resolution, more of these emissions are probably erroneously attributed to North Korea. Simulated mixing ratios are very similar for these two inversions. For instance, the squared Pearson correlation coefficients between the observations and the a posteriori model results (r_b^2) values for Gosan, Hateruma and Cape Ochi-ishi change by only 0.001–0.009 when degrading the resolution to 1° × 1°.

The influence of the number of grid boxes on the inversion results was tested by changing the fraction of boxes subdivided in each grid refinement step. In our standard set-up, we used 2454 boxes. For sensitivity tests, we also used seven different numbers varying of boxes from 546 to 5323 (the coarsest and finest inversion geometry maps are shown in Fig. S4 in the Supplement). The skill of the model in terms of reproducing the observations does not change much, e.g., the r_b^2 values are within 0.446–0.453, 0.571–0.583 and 0.751–0.759 for Gosan, Hateruma and Cape Ochi-ishi, respectively. The emission estimates for larger countries are also stable, while relative differences are larger for smaller countries. Tests showed that the a posteriori emission distribution patterns remained relatively stable when more than about 1500 boxes were used. Thus, we chose about 2500 boxes for our inversions.

ACPD
13, 21003–21040, 2013

3.4 Station network

Inverse modeling benefits from using data from several stations, which allow "viewing" a certain emission region from different angles (Stohl et al., 2010). Inversion results may be quite sensitive to adding or removing a station. Therefore, we tested the influence of the number of stations on the a posteriori SF_6 emissions in East Asia. Figure 3 shows national a priori emissions in each year and the corresponding a posteriori emissions from the reference inversion but using one, two or three stations in East Asia (Mace Head and Trinidad Head were used in all these tests). The changes from the a priori to the a posteriori emissions are generally less strong when only one station is used than when more than one station is used in the inversion. In particular, if all a posteriori emissions from single-station inversions are averaged, the change is smaller than that of the 3-station inversion. This is because with only one station there are fewer observation data to constrain the problem, so the inversion will in general remain closer to the a priori. However, in certain cases, the change can be stronger for single-station cases, e.g., the inversion using only Hateruma data in 2010 produces a posteriori emissions for China that are even slightly larger than the 3-station inversion result.

The impact of the different stations for the national emission estimates is quite different. A posteriori emissions for China and the Taiwan region when using only Hateruma data, for instance, are quite close to the corresponding 3-station result, while using only Gosan or Cape Ochi-ichi data yields a posteriori emissions much closer to the a priori values. This is probably due to the fact that footprint emission sensitivity values in Taiwan and southern China are highest for Hateruma (see Fig. 1). Overall, however, the changes are quite consistent. For instance, the emissions from China and Japan are increased for all inversion setups and for all years (with one exception for China).

ACPD
13, 21003–21040, 2013

3.5 Meteorological input data

To evaluate the influence of meteorological input data resolution, $0.25^\circ \times 0.25^\circ$ ECMWF data for East Asia (100° E to 150° E, 10° N to 50° N) were nested (termed "Nest_ECMWF") into the global $1.0^\circ \times 1.0^\circ$ ECMWF data used without nesting for our reference inversion (termed "ECMWF"). The Nest_ECMWF simulations generally improve the model performance compared to the observations in terms of bias, RMSE and correlation obtained for simulated vs. observed mixing ratios at the three stations (Table S4 in the Supplement). This holds both for a priori and a posteriori results. For example, in the ECMWF case (Nest_ECMWF case) the r_b^2 values are 0.45 (0.49), 0.58 (0.65) and 0.76 (0.77) for Gosan, Hateruma and Cape Ochi-ishi, respectively. However, a posteriori national emission totals are similar (Table S5), e.g. 2312 (ECMWF) and 2355 (Nest_ECMWF) Mg yr^{-1} for China, and there is a difference of only 3 % for total emissions from East Asia. Thus, while dispersion model results are slightly better with nested data, the national emission totals obtained from the inversion relatively stable. Therefore, only global data were used for our seven-year inversion.

Results for inversions using CFSR and FNL data are also shown in Table S4 and Table S5 in the Supplement. There is no one data set that is consistently better than the others. The performance statistics show that for Gosan and Cape Ochi-ishi, the ECMWF data yields best results, while for Hateruma, the FNL data seems to work better. However, even for a given site the best performing data set changes with time. For instance, Fig. 4 shows the mixing ratio timeseries for Hateruma in 2008 and an example of emission sensitivities for highlighted cases is shown in Fig. S5 in the Supplement. Overall, ECMWF simulations performed slightly better than the other data sets but only the Nest_ECMWF simulations give the best results for almost all stations and for almost all statistical parameters. It is difficult to say what exactly causes the different model performances for the non-nested cases. One reason may be the better vertical resolution of the ECMWF data (92 levels compared to 37 and 26 levels for CSFR and FNL). Temporal resolution may be another factor. While ECMWF and

ACPD
13, 21003–21040, 2013

CFSR data were used with 3 h resolution, the FNL data set is 6-hourly. Certainly there are many other differences between the different meteorological data sets such as the underlying physical model and data assimilation scheme
ldots.

3.6 Seasonal variability

One of the sources of uncertainty in our inversion set-up is the assumption that emissions are constant over the target interval for which the inversion is performed. However, this may not be the case. Therefore, we have run seasonal inversions for the periods winter (December, January, February), spring (March, April, May), summer (June, July, August) and fall (September, October, November). For these inversions – and also for the whole-year inversion used for comparison – the number of emission boxes was reduced to about 1500 because of the reduced number of measurements. Five-year seasonal variations of SF_6 a posteriori emissions for each East Asian country show that there is no regular seasonality of the retrieved SF_6 emissions (Fig. 5). For example, for China, in 2007, the inferred emissions are highest in summer, while in 2011, the emissions in summer are the lowest. This irregular variation of emissions is the same in the other five countries/regions. This is not very surprising, because no seasonality is expected for the major SF_6 source categories.

Figure 5 shows that the average of the a posteriori emissions from four seasonal inversions is close to the a posteriori emissions from the whole-year inversion for the same year. For the years 2007–2011, the relative differences between the mean of the seasonal inversions and the reference inversion are -7 ± 4 % for China, 2 ± 17 % for the Taiwan region, -18 ± 35 % for North Korea, 8 ± 13 % for South Korea, -6 ± 8 % for Japan and -6 ± 2 % for East Asia.

ACPD
13, 21003–21040, 2013

3.7 Overview of sensitivity tests

Table 2 presents an overview of the uncertainties of national emissions obtained from the different sensitivity tests for the year 2008. For test i, we report the relative uncertainty U_i as the standard deviation of the a posteriori emissions divided by the mean of the ensemble inversions in test i. Assuming that the uncertainties from N sensitivity tests performed are independent from each other, we report the total relative uncertainty as $U = \sqrt{\sum_{i=1}^{N} U_i^2}$. Table 2 shows that the largest uncertainties are due to the a priori emissions used and their uncertainty, the station network, as well as the meteorological input data. Much lower uncertainties are due to seasonal emission variability, inversion geometry, inversion resolution and measurement scale. It is also evident that relative uncertainties are larger for countries with smaller emissions than for countries with larger emissions. Although uncertainties may be slightly different for other years than the tested year 2008, we apply these uncertainties to the national emission estimates for all years. It should also be noticed that these uncertainties do not include possibly systematic other errors, e.g., certain possible model biases like under- or overestimation of boundary layer heights which may be important especially for countries like China where reported stochastic errors are small.

4 National total emissions and emission distribution

4.1 National emissions

National emissions as obtained from the inversion are reported in Table 3, with uncertainties (indicated by ± values) derived from the overall relative uncertainties as obtained in the sensitivity tests. We consider these uncertainty estimates as more realistic than the smaller uncertainties obtained from error propagation in a single reference inversion. Measurement statistics and inversion performance for the period 2006–2012

ACPD
13, 21003–21040, 2013

are shown in Table S6 in the Supplement, and timeseries of the measured and simulated SF_6 mixing ratios for 2011 are shown as an example in Fig. S6 in the Supplement.

Comparisons of our estimates with other published estimates are shown in Fig. 6 for China, our best estimate for 2008, $2385 \pm 411\,Mg\,yr^{-1}$, is larger than the estimate of $1300\,(930–1700)\,Mg\,yr^{-1}$ reported by Kim et al. (2010) and agrees within uncertainty with the value of $2383\,(1867–2865)\,Mg\,yr^{-1}$ for 2007–2009 reported by Rigby et al. (2011). Our estimate for 2007 is also much larger than the estimate of Vollmer et al. (2009) for the same year, although the emissions of other halocarbons estimated by Vollmer et al. (2009) are higher than those reported in other studies (Stohl et al., 2010; Li et al., 2011). Compared with the bottom-up estimates of Fang et al. (2013) and EDGAR (2011), our estimates are slightly higher (especially for years 2007–2009) but with consistent emission trends.

For the Taiwan region, the a posteriori emissions are consistent with the estimated emissions by Rigby et al. (2011), but are about two times higher than the bottom-up estimates in the Second National Communication of Taiwan for the years 2007 and 2008 (Taiwan, 2011). For South Korea, the inversion results are lower than bottom-up estimates in the South Korea National Communication (Republic of Korea, 2012). However, our estimates for the years 2008 and 2009 are about twice as high as estimates by Li et al. (2011) and Rigby et al. (2011). This is not due to a too high a priori adopted in our inversion because a posteriori values of the same magnitude were still obtained even with the a priori value cut by 50 %. For Japan, our estimates agree within the uncertainty range with the ratio-method estimates of Li et al. (2011) and the inversion estimates of Rigby et al. (2011). The reported emissions to UNFCCC and EDGAR estimates are lower than our estimates for Japan.

The emission trend was very different in individual East Asian countries during the 2006–2012 period. For Japan, one of the Annex-I countries under UNFCCC, inversion results show that its emissions are decreasing except for the year 2011. From 2008 to 2009, there is a relatively large decrease in emissions, which is partly due to a reported reduction of $43\,Mg\,yr^{-1}$ caused by the equipment of SF_6 manufacturing facilities

ACPD
13, 21003–21040, 2013

with recovery/destruction units and reported reductions of 17 Mg yr^{-1} in the magnesium foundry sector and 11 Mg yr^{-1} in the semiconductor manufacture sector in 2009 (GIO, 2012). The emission anomaly in 2011 is very likely caused by the escape into the air of SF_6 enclosed in certain high-voltage electrical insulation equipment due to the damage caused by the Great East Japan Earthquake on 11 March 2011. Seasonal inversions show that the increase is largely due to extraordinarily high emissions in spring, consistent with a source related to the earthquake. Indeed, loss of SF_6 due to earthquake damage was reported by some companies (e.g., Hitachi, 2011).

For China, the posteriori emissions almost doubled during 2006–2012, reflecting a fast increase of SF_6 consumption and emissions in China. Usage of SF_6 in the electrical equipment sector was estimated to have increased from about 820 Mg yr^{-1} in 2001 to 4990 Mg yr^{-1} in 2010, with a bigger leap in the first five years. Usage of SF_6 in the semiconductor manufacturing sector and the magnesium production sector also increased by about four times and the total of these two sectors accounts for one eighth of that in the electrical equipment sector (Fang et al., 2013). Considering the increase of usage during the period 2001–2010 and the delay between its employment and its emissions in the electrical equipment sector, an emission increase during 2006–2012 is expected.

For South Korea, emissions increase slightly from 2006 to 2012, with an exception in 2007. CDM projects with 86 Mg yr^{-1} reduction capacity and additional 64 Mg yr^{-1} reduction capacity were launched in 2010 and in 2011, respectively. Without these CDM reductions, the SF_6 emissions in South Korea would most likely have increased more strongly. For the Taiwan region, Communication to UNFCCC report increasing emissions from 2000–2008 (Taiwan, 2011), and we find a decrease from about the year 2008, suggesting emissions from Taiwan peaked around the year 2008. However, emissions for 2012 are estimated to be much higher than those in previous years. Emissions from North Korea and Mongolia are very small and there are no significant trends. For North Korea, it is possible that some of the emissions are actually due to

ACPD
13, 21003–21040, 2013

South Korean sources close to the border, which could not be correctly attributed by the inversion.

The SF_6 emissions from East Asia as a whole (Fig. 7, upperleft) grew gradually from $2437 \pm 329\,Mg\,yr^{-1}$ in 2006 to $3787 \pm 512\,Mg\,yr^{-1}$ in 2009 and stabilized afterwards. The global SF_6 emissions for the period 2006–2008 have likely increased almost linearly (see Table S1) but at smaller relative growth rates than East Asian emissions. Contribution from emissions in East Asia to the global totals increased from 38 ± 5 % in 2006 to 49 ± 7 % in 2009. Based on extrapolated global emissions (see sub-Sect. 2.4), the contributions of East Asia to the global totals stabilized between 49 ± 7 % and 45 ± 6 % for the period 2009–2012.

The major contribution to East Asian emissions is from China (Fig. 7, upperright), accounting for 58–72 % depending on the year, followed by South Korea (9–19 %), Japan (5–16 %) and the Taiwan region (4–7 %), while emissions from North Korea and Mongolia together contribute less than 3 %. Taken on a per-capita basis, SF_6 emissions in China and Japan are close to the global average (Fig. 7, bottom). On the other hand, per-capita emissions from South Korea and Taiwan are more than five times than the global per-capita emissions.

4.2 Spatial emission distribution and Chinese provincial emissions

Maps of a posteriori emission distributions for 2008 and 2012, as well as of the difference between these two years, are shown in Fig. 8. The highest a posteriori flux densities are in South Korea where the Liquid Crystal Display (LCD) sector and electrical equipment sector are two important emission sources. Several abatement CDM projects were launched in the LCD sector in 2010 and 2011, so it is seen that emissions from some of boxes containing LCD factories have decrease afterwards. We have to consider the compensation by emission increases from other sources located in the same boxes. For the Taiwan region, the emissions are higher in the west than in the east, as the population is denser and there is more industry along the western coastline. For Japan, high emission fluxes occur in the regions of Tokyo, Osaka and Nagoya.

ACPD
13, 21003–21040, 2013

For China, high emissions are concentrated in Liaoning and Jilin (Northeast China), Beijing, Hebei, Shanxi and Henan (North China), Shandong, Jiangsu, Shanghai and Zhejiang (East China) and Sichuan (Southwest China) provinces.

The locations of factories known to have produced SF_6 around the year 2008 (Xiao, 2010; Cheng, 2010) are also marked in Fig. 8. Almost all Chinese factories are shown on the map, but this was not used as a priori information in the inversion. While loss during SF_6 production is only one source of SF_6, estimated as 7.5 % of inventoried total emissions in China (Fang et al., 2013), most of the factory locations are associated with high a posteriori emissions by the inversion. However, in China, emissions from electrical equipment dominate, accounting for more than 70 % of national totals based on the estimates by Fang et al. (2013). Hundreds of thousands of individual devices containing SF_6 have been reported in the yearbook (CEPP, 2010), leading to widespread distribution of SF_6 emission sources.

During 2008–2012, emission distribution patterns changed differently for different countries (Fig. 8). For South Korea and the Taiwan region, emissions in some parts decreased, compensated by increases in some other parts. In Japan and North Korea we see decreases in most parts, while emission distributions in Mongolia did not change much. For China as a whole, the emissions increased gradually, but with large regional differences (Fig. 9). Emissions in South China decreased slightly during 2008–2010 and increased again afterwards, while emissions in Northwest and North China reached a peak around the year 2009. Like the emissions in whole China, emissions in East, Middle and Northeast China grew gradually during almost the whole period. Fluctuant emissions are observed for Southwest China. These regional differences should be caused by changes of provincial SF_6 usage and by shifts of usage among different sectors, but right now little information of provincial usage for each sector is available.

ACPD
13, 21003–21040, 2013

5 Conclusions

We have performed a large number of sensitivity tests to quantify the uncertainties associated with our inversion set-up. We found that the most important sources of uncertainty associated with the inversions are related to the a priori emissions used and their assumed uncertainty, the station network as well as the meteorological input data. Much lower uncertainties are due to seasonal emission variability, inversion geometry, inversion resolution and measurement calibration scale. The overall relative uncertainties of the national a posteriori emissions are 184 %, 17 %, 49 %, 106 %, 26 % and 17 % for Mongolia, China, the Taiwan region, North Korea, South Korea and Japan, respectively.

Based on sensitivity tests, we employed the optimal parameters in our inversion setup and performed yearly inversions for the period 2006–2012. Results show that the SF_6 emissions from East Asia as a whole grew gradually from $2437 \pm 329\,Mg\,yr^{-1}$ in 2006 to $3787 \pm 512\,Mg\,yr^{-1}$ in 2009 and stabilized afterwards. Contributions from East Asia to global emissions are estimated to be between 38 ± 5 % and 49 ± 7 % in different years. The major contributor to the East Asian totals is China (58–72 % depending on the year), followed by South Korea (9–19 %), Japan (5–16 %) and the Taiwan region (4–7 %), while emissions from North Korea and Mongolia together were less than 3 % of the total. Chinese emissions increased from $1420 \pm 245\,Mg\,yr^{-1}$ in 2006 to $2741 \pm 472\,Mg\,yr^{-1}$ in 2009 and did not change much afterwards. Emissions from South Korea increased from $463 \pm 122\,Mg\,yr^{-1}$ in 2006 to $657 \pm 172\,Mg\,yr^{-1}$ in 2012, while emissions from the Taiwan region and Japan have decreased overall. The per-capita SF_6 emissions in South Korea and the Taiwan region are more than five times the global per-capita emissions, while per-capita emissions for China, North Korea and Japan are close to global average. Emission spatial distributions changed differently in different parts of East Asia. For example, while the total Chinese emissions increased gradually, there were large regional differences.

ACPD
13, 21003–21040, 2013

Supplementary material related to this article is available online at http://www.atmos-chem-phys-discuss.net/13/21003/2013/acpd-13-21003-2013-supplement.pdf.

Acknowledgements. We acknowledge use of ECMWF, CFSR and FNL meteorological data. Atmospheric observations at Hateruma and Cape Ochi-ishi stations were supported by the Global Environment Fund (Ministry of the Environment of Japan). Measurements at Gosan station were supported by the National Research Foundation of Korea (NRF, No. 2010-0029119). We thank Atmospheric Chemistry Research Group, University of Bristol (UB), UK and Scripps Institution of Oceanography (SIO), University of California, United States, for running the Mace Head and Trinidad Head AGAGE stations, respectively, and SIO for providing the calibrations for these two stations and Gosan. We acknowledge Jens Mühle (SIO) and Christina Harth (SIO) for their great contribution to the intercalibration between NIES-2008 and SIO-2005. We also acknowledge use of EDGAR and UNFCCC emission data, and CIESIN gridded population data. The financial support provided by China Scholarship Council (No. 201206010235) during a one-year visit of Xuekun Fang in Norwegian Institute for Air Research is gratefully acknowledged. The Norwegian Research Council also provided partial support through the SOGG-EA project (No. 193774).

References

CEPP: China Electric Power Yearbook, China Electric Power Press (CEPP), Beijing, China, 2010, (in Chinese).

Cheng, H.: Competitive strength and market analysis of electronic chemicals and special gas containing fluorine, Chemical Production and Technology, 17, 1–7, 2010, (in Chinese with English abstract).

China: Second National Communication on Climate Change of The People's Republic of China, National Development and Reform Commission of China, Beijing, China, 2012.

CIESIN: Gridded Population of the World: Future Estimates (GPWFE), available at: http://sedac.ciesin.columbia.edu/data/collection/gpw-v3 (last access: 7 November 2012), Center for International Earth Science Information Network (CIESIN), 2005.

ACPD
13, 21003–21040, 2013

Democratic People's Republic of Korea: DPRK's First National Communication Under the Framework Convention on Climate Change, Ministry of Land and Environment Protection, Democratic People's Republic of Korea, 2000.

EDGAR: Emission Datebase for Global Atmospheric Research (EDGAR), release version 4.2, available at: http://edgar.jrc.ec.europa.eu (last access: 22 March 2012), European Commission, Joint Research Centre (JRC)/Netherlands Environmental Assessment Agency (PBL), 2011.

Enomoto, T., Yokouchi, Y., Izumi, K., and Inagaki, T.: Development of an analytical method for atmospheric halocarbons and its application to airborne observation, J. Jpn. Soc. Atmos. Environ., 1–8, 2005, (in Japanese).

Fang, X., Hu, X., Janssens-Maenhout, G., Wu, J., Han, J., Su, S., Zhang, J., and Hu, J.: Sulfur hexafluoride (SF_6) emission estimates for China: an inventory for 1990–2010 and a projection to 2020, Environ. Sci. Technol., 47, 3848–3855, doi:10.1021/es304348x, 2013.

Forster, P., Ramaswamy, V., Artaxo, P., Berntsen, T., Betts, R., Fahey, D. W., Haywood, J., Lean, J., Lowe, D. C., Myhre, G., Nganga, J., Prinn, R., Raga, G., Schulz, M., and Dorland, R. V.: Changes in atmospheric constituents and in radiative forcing, in: Climate Change 2007: The Physical Science Basis. Contribution of Working Group I to the Fourth Assessment Report of the Intergovernmental Panel on Climate Change, edited by: Solomon, S., Qin, D., Manning, M., Chen, Z., Marquis, Z., Avery, K. B., Tignor, M., and Miller, H. L., Cambridge University Press, Cambridge, UK, 129–234, 2007.

GIO: National Greenhouse Gas Inventory Report of Japan 2012, Greenhouse Gas Inventory Office of Japan (GIO), Center for Global Environmental Research (CGER), National Institute for Environmental Studies (NIES), Ministry of the Environment, Japan, 2012.

Hitachi: Report on the Great East Japan Earthquarke: Global Warming Prevention, Hitachi Cable, Ltd., Japan, 2011.

Janssens-Maenhout, G., Diego, V. P., and Marilena Muntean, G.: Global emission inventories in the Emission Database for Global Atmospheric Research (EDGAR) – Manual (I). Gridding: EDGAR Emissions Distribution on Global Gridmaps, Publications Office of the European Union, Luxembourg, 2013.

Keller, C. A., Hill, M., Vollmer, M. K., Henne, S., Brunner, D., Reimann, S., O'Doherty, S., Arduini, J., Maione, M., Ferenczi, Z., Haszpra, L., Manning, A. J., and Peter, T.: European emissions of halogenated greenhouse gases inferred from atmospheric measurements, Environ. Sci. Technol., 46, 217–225, doi:10.1021/es202453j, 2012.

ACPD
13, 21003–21040, 2013

Kim, J., Li, S., Kim, K. R., Stohl, A., Mühle, J., Kim, S. K., Park, M. K., Kang, D. J., Lee, G., Harth, C. M., Salameh, P. K., and Weiss, R. F.: Regional atmospheric emissions determined from measurements at Jeju Island, Korea: halogenated compounds from China, Geophys. Res. Lett., 37, L12801, doi:10.1029/2010GL043263, 2010.

Levin, I., Naegler, T., Heinz, R., Osusko, D., Cuevas, E., Engel, A., Ilmberger, J., Langenfelds, R. L., Neininger, B., Rohden, C. v., Steele, L. P., Weller, R., Worthy, D. E., and Zimov, S. A.: The global SF_6 source inferred from long-term high precision atmospheric measurements and its comparison with emission inventories, Atmos. Chem. Phys., 10, 2655–2662, doi:10.5194/acp-10-2655-2010, 2010.

Li, S., Kim, J., Kim, K. R., Mühle, J., Kim, S. K., Park, M. K., Stohl, A., Kang, D. J., Arnold, T., Harth, C. M., Salameh, P. K., and Weiss, R. F.: Emissions of halogenated compounds in East Asia determined from measurements at Jeju Island, Korea, Environ. Sci. Technol., 45, 5668–5675, doi:10.1021/Es104124k, 2011.

Miller, B. R., Weiss, R. F., Salameh, P. K., Tanhua, T., Greally, B. R., Mühle, J., and Simmonds, P. G.: Medusa: a sample preconcentration and GC/MS detector system for in situ measurements of atmospheric trace halocarbons, hydrocarbons, and sulfur compounds, Anal. Chem., 80, 1536–1545, doi:10.1021/Ac702084k, 2008.

Mongolia: Mongolia Second National Communication Under the United Nations Framework Convention on Climate Change, Ministry of Nature, Environment and Tourism, Ulaanbaatar, Mongolia, 2010.

Olivier, J. G. J., Van Aardenne, J. A., Dentener, F., Ganzeveld, L., and Peters, J. A. H. W.: Recent trends in global greenhouse gas emissions: regional trends and spatial distribution of key sources, in: Non-CO_2 Greenhouse Gases (NCGG-4), edited by: v. Amstel, A., Millpress, Rotterdam, the Netherlands, 325–330, 2005.

Prinn, R. G., Weiss, R. F., Fraser, P. J., Simmonds, P. G., Cunnold, D. M., Alyea, F. N., O'Doherty, S., Salameh, P., Miller, B. R., Huang, J., Wang, R. H. J., Hartley, D. E., Harth, C., Steele, L. P., Sturrock, G., Midgley, P. M., and McCulloch, A.: A history of chemically and radiatively important gases in air deduced from ALE/GAGE/AGAGE, J. Geophys. Res., 105, 17751–17792, doi:10.1029/2000jd900141, 2000.

Ravishankara, A. R., Solomon, S., Turnipseed, A. A., and Warren, R. F.: Atmospheric lifetimes of long-lived halogenated species, Science, 259, 194–199, 1993.

ACPD
13, 21003–21040, 2013

Republic of Korea: Korea's Third National Communication Under the United Nations Framework Convention on Climate Change, Ministry of Environment, Seoul, The Republic of Korea, 2012.

Rigby, M., Mühle, J., Miller, B. R., Prinn, R. G., Krummel, P. B., Steele, L. P., Fraser, P. J., Salameh, P. K., Harth, C. M., Weiss, R. F., Greally, B. R., O'Doherty, S., Simmonds, P. G., Vollmer, M. K., Reimann, S., Kim, J., Kim, K.-R., Wang, H. J., Olivier, J. G. J., Dlugokencky, E. J., Dutton, G. S., Hall, B. D., and Elkins, J. W.: History of atmospheric SF_6 from 1973 to 2008, Atmos. Chem. Phys., 10, 10305–10320, doi:10.5194/acp-10-10305-2010, 2010.

Rigby, M., Manning, A. J., and Prinn, R. G.: Inversion of long-lived trace gas emissions using combined Eulerian and Lagrangian chemical transport models, Atmos. Chem. Phys., 11, 9887–9898, doi:10.5194/acp-11-9887-2011, 2011.

Stohl, A., Hittenberger, M., and Wotawa, G.: Validation of the Lagrangian particle dispersion model FLEXPART against large-scale tracer experiment data, Atmos. Environ., 32, 4245–4264, doi:10.1016/s1352-2310(98)00184-8, 1998.

Stohl, A., Forster, C., Frank, A., Seibert, P., and Wotawa, G.: Technical note: The Lagrangian particle dispersion model FLEXPART version 6.2, Atmos. Chem. Phys., 5, 2461–2474, doi:10.5194/acp-5-2461-2005, 2005.

Stohl, A., Seibert, P., Arduini, J., Eckhardt, S., Fraser, P., Greally, B. R., Lunder, C., Maione, M., Mühle, J., O'Doherty, S., Prinn, R. G., Reimann, S., Saito, T., Schmidbauer, N., Simmonds, P. G., Vollmer, M. K., Weiss, R. F., and Yokouchi, Y.: An analytical inversion method for determining regional and global emissions of greenhouse gases: Sensitivity studies and application to halocarbons, Atmos. Chem. Phys., 9, 1597–1620, doi:10.5194/acp-9-1597-2009, 2009.

Stohl, A., Kim, J., Li, S., O'Doherty, S., Mühle, J., Salameh, P. K., Saito, T., Vollmer, M. K., Wan, D., Weiss, R. F., Yao, B., Yokouchi, Y., and Zhou, L. X.: Hydrochlorofluorocarbon and hydrofluorocarbon emissions in East Asia determined by inverse modeling, Atmos. Chem. Phys., 10, 3545–3560, doi:10.5194/acp-10-3545-2010, 2010.

Taiwan: Second National Communication of the Republic of China (Taiwan) Under the United Nations Framework Convention on Climate Change Executive Summary, 2011.

Tohjima, Y., Machida, T., Utiyama, M., Katsumoto, M., Fujinuma, Y., and Maksyutov, S.: Analysis and presentation of in situ atmospheric methane measurements from Cape Ochi-ishi and

ACPD
13, 21003–21040, 2013

Hateruma Island, J. Geophys. Res., 107, ACH 8-1–ACH 8–11, doi:10.1029/2001jd001003, 2002.

UN: Kyoto Protocol to the United Nations Framework Convention on Climate Change, United Nations, 1998.

UNFCCC: Flexible GHG Data Queries, available at: http://unfccc.int/di/FlexibleQueries.do (last access: 21 December 2012), United Nations Framework Convention on Climate Change (UNFCCC), 2012a.

UNFCCC: United Nations Framework Convention on Climate Change: Clean Development Mechanism (CDM), available at: http://cdm.unfccc.int/Projects/projsearch.html (last access: 20 December 2012), 2012b.

Vollmer, M. K., Zhou, L. X., Greally, B. R., Henne, S., Yao, B., Reimann, S., Stordal, F., Cunnold, D. M., Zhang, X. C., Maione, M., Zhang, F., Huang, J., and Simmonds, P. G.: Emissions of ozone-depleting halocarbons from China, Geophys. Res. Lett., 36, L15823, doi:10.1029/2009gl038659, 2009.

Xiao, M. L.: Development analysis of domestic sulfur hexafluoride industry, Chemical Propellants & Polymeric Materials, 8, 65–67, 2010, (in Chinese with English abstract).

Yokouchi, Y., Taguchi, S., Saito, T., Tohjima, Y., Tanimoto, H., and Mukai, H.: High frequency measurements of HFCs at a remote site in east Asia and their implications for Chinese emissions, Geophys. Res. Lett., 33, L21814, doi:10.1029/2006GL026403, 2006.

ACPD
13, 21003–21040, 2013

Table 1. List of the measurement stations, corresponding coordinates, the operating institutions and the period of available data used in this study.

Station	Longitude	Latitude	Altitude	Institution	Calibration scale	Period
Gosan, South Korea	126.17	33.28	72	SNU (AGAGE)	SIO-2005	Jan 2008–Dec 2012
Hateruma, Japan	123.81	24.06	47	NIES	NIES-2008	Jan 2006–Dec 2012
Cape Ochi-ishi, Japan	145.50	43.16	96	NIES	NIES-2008	Aug 2006–Dec 2012
Mace Head, Ireland	−9.90	53.33	25	UB (AGAGE)	SIO-2005	Jan 2006–Dec 2011
Trinidad Head, USA	−124.15	41.05	140	SIO (AGAGE)	SIO-2005	Jan 2006–Dec 2011

ACPD
13, 21003–21040, 2013

Table 2. Relative uncertainties of a posteriori SF_6 emissions in East Asia as obtained from the different sensitivity tests, as well as total uncertainty assuming that the individual errors are independent.

	Factors	Relative uncertainty						
		Mongolia	China	Taiwan region	North Korea	South Korea	Japan	East Asia
1	Measurement scale	0 %	1 %	1 %	0 %	0 %	1 %	1 %
2	A priori information	87 %	9 %	20 %	38 %	16 %	6 %	7 %
3	Emission uncertainty	60 %	10 %	3 %	44 %	10 %	1 %	6 %
4	Inversion geometry	45 %	2 %	6 %	19 %	1 %	1 %	2 %
5	Inversion resolution	0 %	0 %	8 %	17 %	5 %	0 %	0 %
6	Station network	106 %	8 %	17 %	56 %	14 %	6 %	4 %
7	Meteorological data	77 %	5 %	40 %	47 %	9 %	12 %	7 %
8	Seasonal variability	61 %	6 %	6 %	43 %	1 %	9 %	5 %
	Overall	184 %	17 %	49 %	106 %	26 %	17 %	14 %

ACPD
13, 21003–21040, 2013

Table 3. SF_6 emissions ($Mg\,yr^{-1}$) per country/region for the period 2006–2012. Results are shown for the mean a posteriori emissions from the inversion ensemble, and the corresponding uncertainties estimated based on the overall relative uncertainties in Table 2.

	Mongolia	China	Taiwan region	North Korea	South Korea	Japan	East Asia
2006	8 ± 15	1420 ± 245	118 ± 58	45 ± 48	463 ± 122	383 ± 67	2437 ± 329
2007	17 ± 31	2145 ± 370	215 ± 105	41 ± 43	288 ± 76	349 ± 61	3055 ± 413
2008	2 ± 4	2385 ± 411	239 ± 117	76 ± 81	532 ± 140	309 ± 54	3542 ± 479
2009	36 ± 66	2741 ± 472	184 ± 90	65 ± 69	546 ± 143	215 ± 38	3787 ± 512
2010	64 ± 118	2549 ± 439	208 ± 102	36 ± 38	586 ± 154	172 ± 30	3616 ± 489
2011	46 ± 85	2827 ± 487	177 ± 87	67 ± 71	584 ± 153	360 ± 63	4061 ± 549
2012	14 ± 26	2868 ± 494	301 ± 148	38 ± 40	657 ± 172	185 ± 32	4063 ± 549

ACPD
13, 21003–21040, 2013

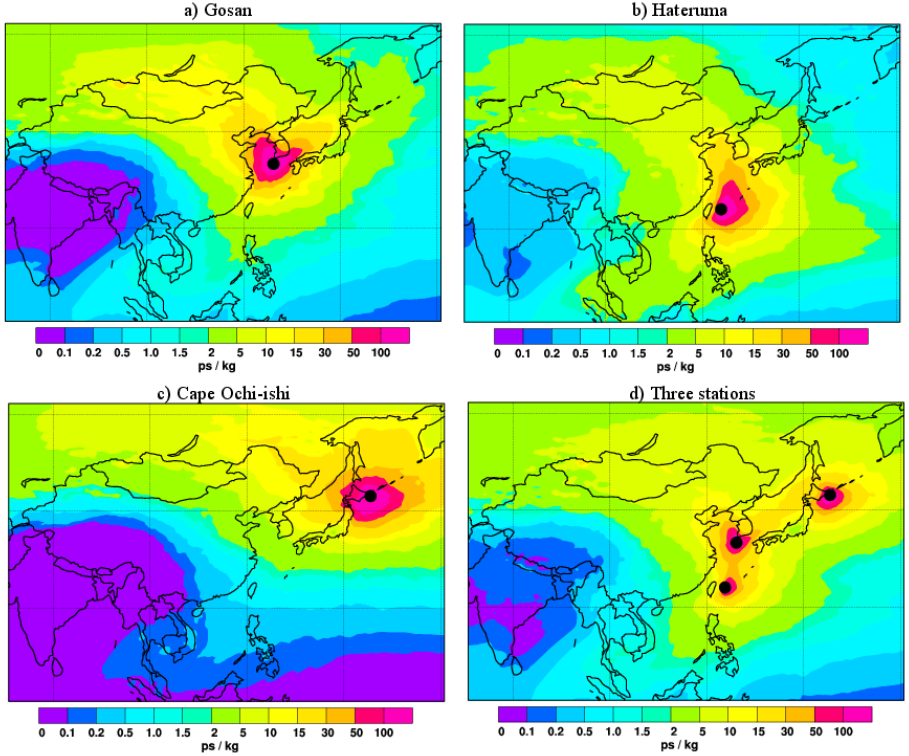

Fig. 1. Footprint emission sensitivity obtained from FLEXPART 20 day backward simulations based on ECMWF input data averaged for the period 2006–2012 for Gosan **(a)**, Hateruma **(b)**, Cape Ochi-shi **(c)** and all three stations **(d)**. Black dots represent the corresponding measurement stations.

ACPD
13, 21003–21040, 2013

Sulfur hexafluoride (SF_6) emissions in East Asia determined by inverse modeling

X. Fang et al.

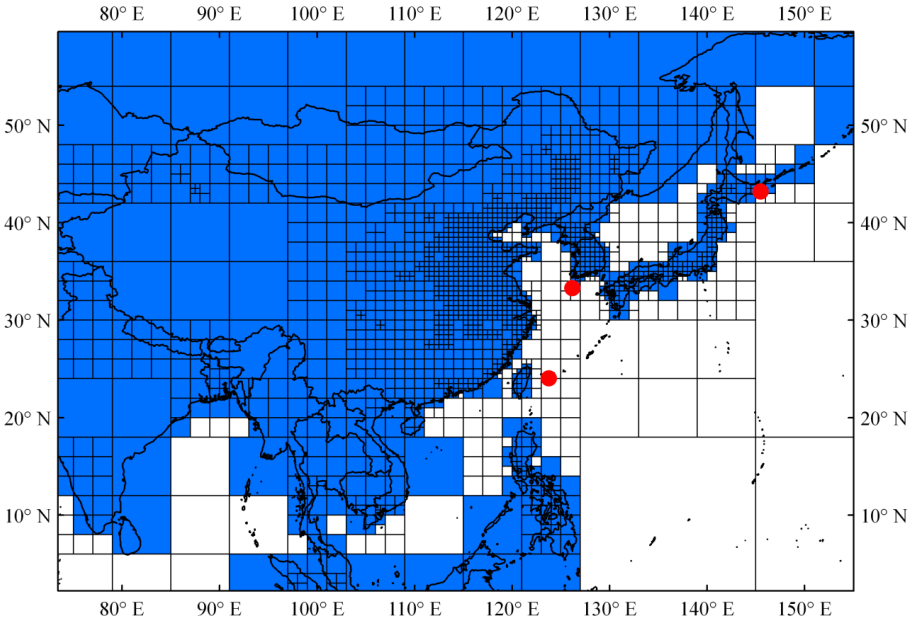

Fig. 2. Map showing a zoom-in over East Asia of the variable-resolution grid (highest resolution 0.5° × 0.5°) used for the inversion. The red dots denote the measurement stations. Blue boxes are considered in the inversion process and white boxes are not used.

ACPD
13, 21003–21040, 2013

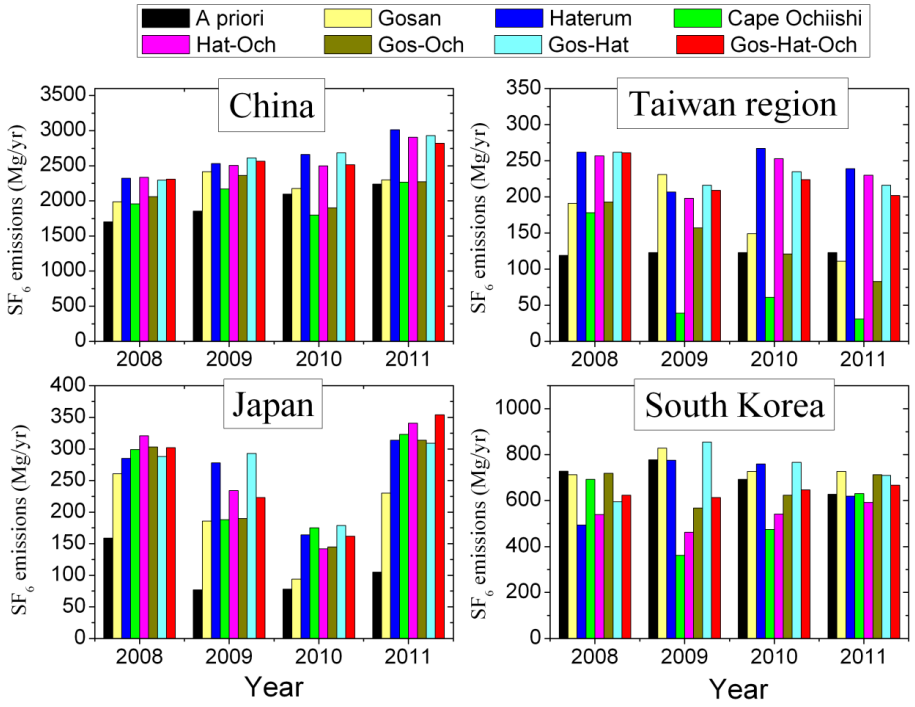

Fig. 3. A priori and a posteriori national SF_6 emissions in East Asia for the years 2008–2011. A posteriori results are from the reference inversion but using measurement data from only one, two or all three East Asian measurement stations (Gos = Gosan, Hat = Hateruma and Och = Cape Ochi-ishi).

ACPD
13, 21003–21040, 2013

Sulfur hexafluoride (SF_6) emissions in East Asia determined by inverse modeling

X. Fang et al.

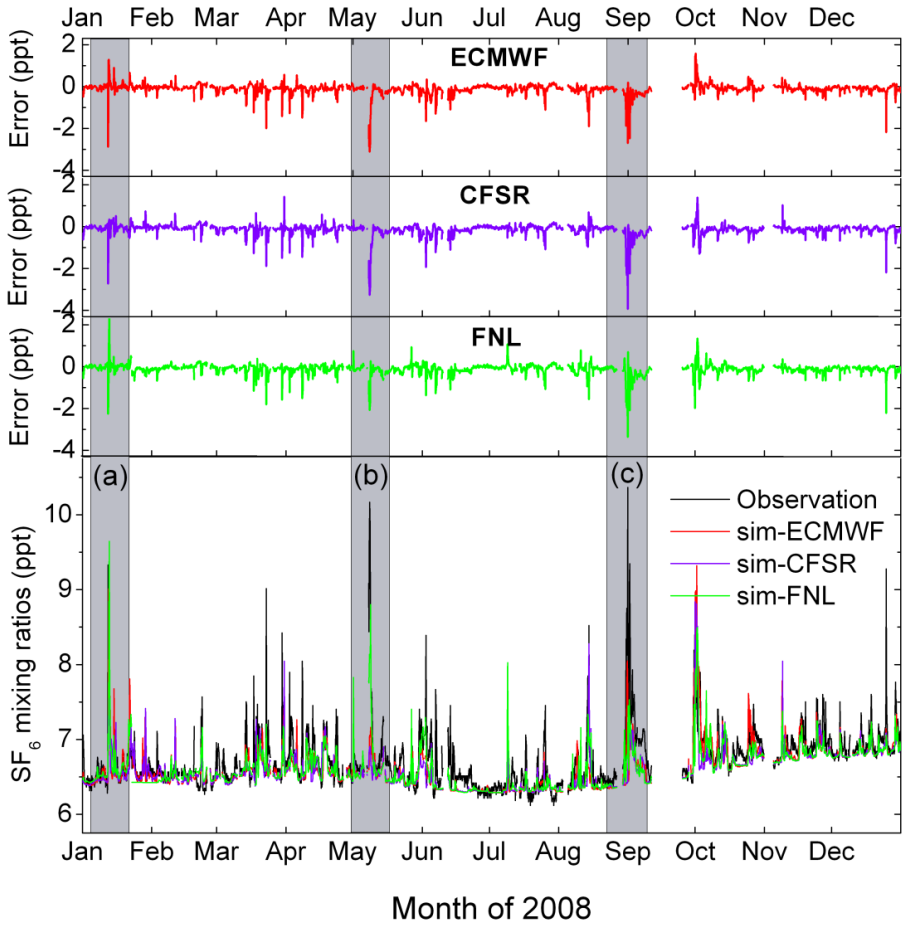

Fig. 4. Observed and simulated SF_6 mixing ratio timeseries at Hateruma station when using ECMWF, CFSR and FNL meteorological data for 2008. Pollution episodes labeled (a), (b) and (c) were best simulated by using CFSR, FNL and ECMWF data set, respectively.

ACPD
13, 21003–21040, 2013

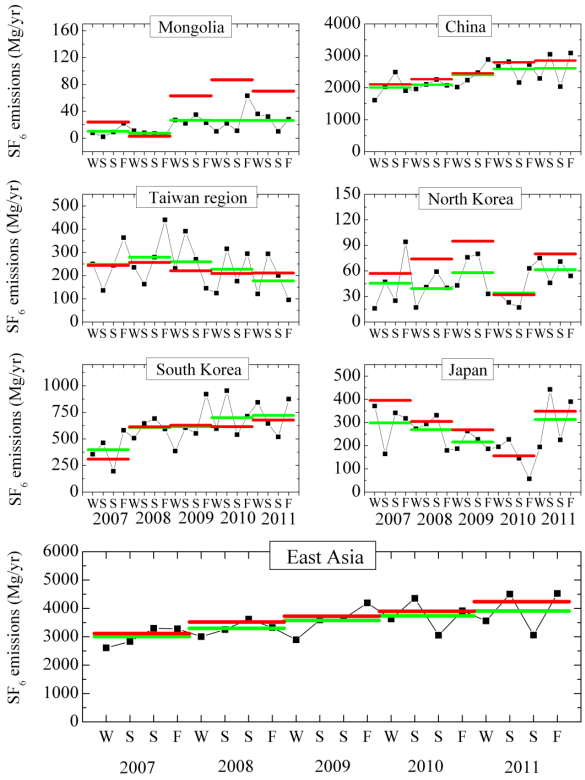

Fig. 5. Seasonal variations of SF_6 a posteriori emissions for each East Asian country for the 2007–2011 period. Black dots denote a posteriori emissions from seasonal inversions; green lines denote an average of a posteriori emissions from four seasonal inversions in each year; red lines denote a posteriori emissions from the reference inversion using the whole-year observation data. W, S, S and F on the X-axis represent winter (December, January, and February), spring (March, April, and May), summer (June, July and August) and fall (September, October and November) in each year, respectively.

ACPD
13, 21003–21040, 2013

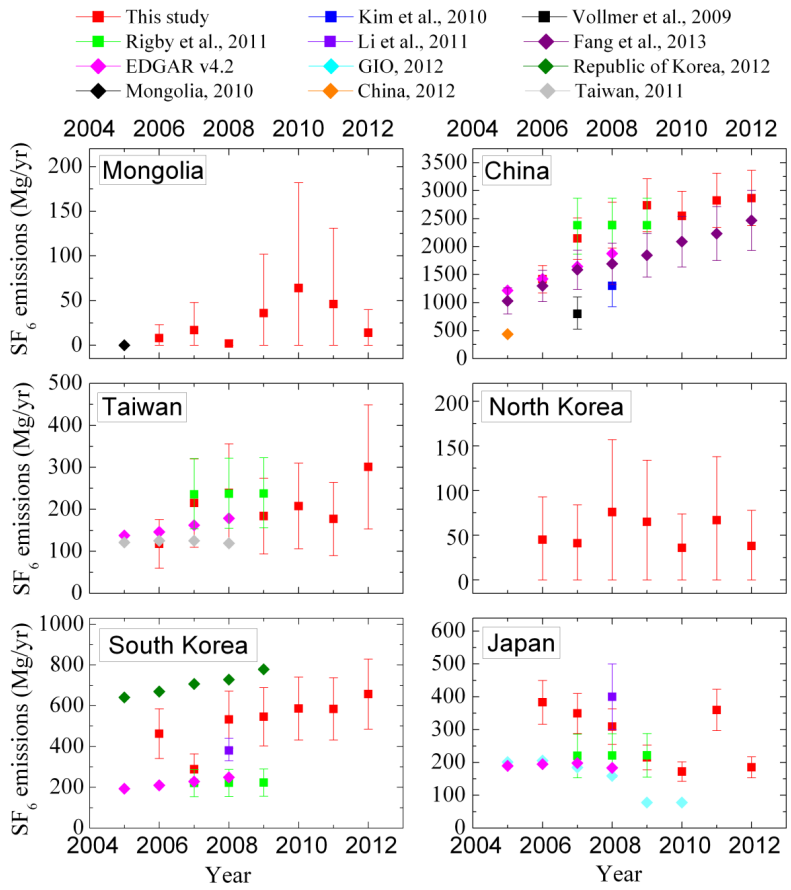

Fig. 6. Comparison of our a posteriori national emission estimates with other published estimates, as specified in the legend at the top. Square symbols denote top-down estimates and diamond symbols denote bottom-up estimates.

ACPD
13, 21003–21040, 2013

Sulfur hexafluoride (SF_6) emissions in East Asia determined by inverse modeling

X. Fang et al.

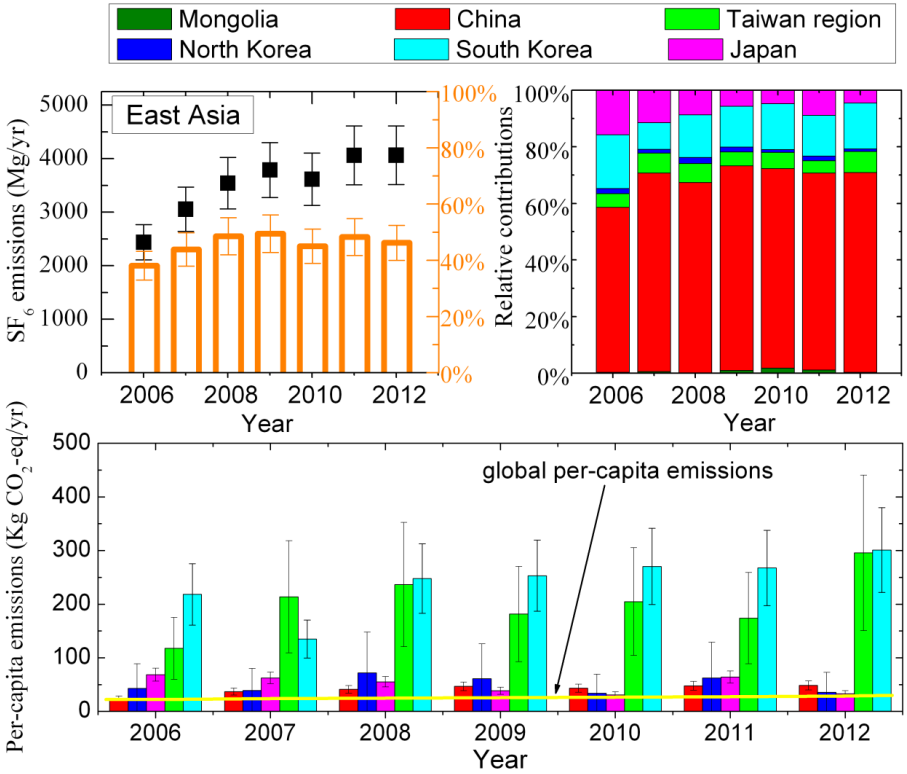

Fig. 7. Global perspective of SF_6 emissions of East Asian countries. The upper left panel shows absolute (black symbols and left Y-axis) and relative contributions (orange symbols and right Y-axis) of emissions in East Asia to the global totals. The upper right panel shows relative contributions of emissions from each country within East Asia. The lower panel shows per-capita emissions for each country, with the yellow line indicating the global average.

ACPD
13, 21003–21040, 2013

Sulfur hexafluoride (SF_6) emissions in East Asia determined by inverse modeling

X. Fang et al.

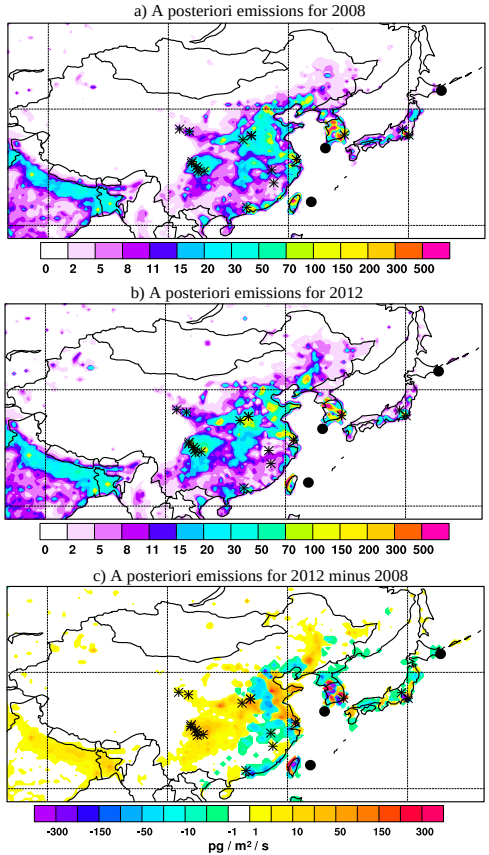

Fig. 8. Maps of the a posteriori SF_6 emissions for 2008 **(a)** and 2012 **(b)**, and difference between a posteriori emissions for 2012 and those for 2008 **(c)**. Black dots denote the location of measurement stations. Asterisks mark the locations of Chinese, South Korean and Japanese factories known to have produced SF_6 in the year 2008. Asterisks mark the locations of factories in East Asia known to have produced SF_6 around the year 2008.

ACPD
13, 21003–21040, 2013

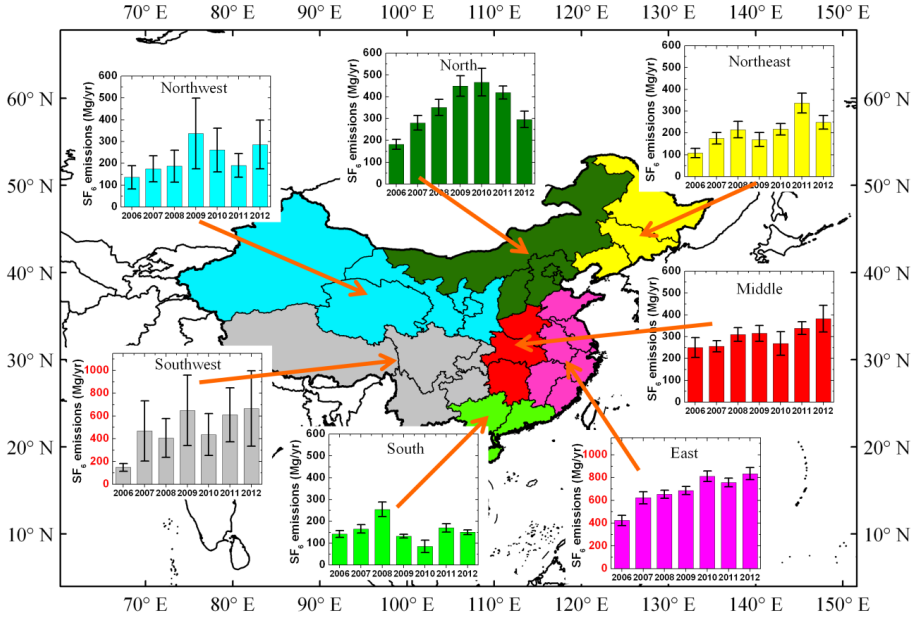

Fig. 9. A posteriori emissions for different regions of China for the 2006–2012 period. Regions of China include North, Northeast, East, South, Southwest, Northwest and Middle China. Note that scales of the Y-axes labeled red in two of the lowermost panels are different from those in other panels.

ACPD
13, 21003–21040, 2013

Sulfur hexafluoride (SF_6) emissions in East Asia determined by inverse modeling

X. Fang et al.